Capacitance electrochemical biosensor based on silicon nitride transducer for TNF-α cytokine detection in artificial human saliva: Heart failure (HF)

Article *in* Talanta · October 2019

DOI: 10.1016/j.talanta.2019.120501

CITATIONS
0

READS
81

6 authors, including:

Mohamed Bahri
Chinese Academy of Sciences
2 PUBLICATIONS **0** CITATIONS
SEE PROFILE

Abdellatif Baraket
Claude Bernard University Lyon 1
78 PUBLICATIONS **377** CITATIONS
SEE PROFILE

Mounir Ben Ali
Higher Institute of Technological Studies of Sousse
73 PUBLICATIONS **712** CITATIONS
SEE PROFILE

Joan Bausells
Spanish National Research Council
224 PUBLICATIONS **2,550** CITATIONS
SEE PROFILE

Talanta 209 (2020) 120501

Contents lists available at ScienceDirect

Talanta

journal homepage: www.elsevier.com/locate/talanta

Capacitance electrochemical biosensor based on silicon nitride transducer for TNF-α cytokine detection in artificial human saliva: Heart failure (HF)

Mohamed Bahri[a,b], Abdoullatif Baraket[c,*], Nadia Zine[c], Mounir Ben Ali[a,b], Joan Bausells[d], Abdelhamid Errachid[c]

[a] NANOMISENE Lab, LR16CRMN01, Centre for Research on Microelectronics and Nanotechnology of Sousse, Technopole of Sousse B.P. 334, Sahloul, 4034, Sousse, Tunisia
[b] University of Sousse, Higher Institute of Applied Sciences and Technology of Sousse,GREENS-ISSAT, Cité Ettafala, 4003, Ibn Khaldoun Sousse, Tunisia
[c] Université de Lyon, Institut des Sciences Analytiques, UMR 5280, CNRS, Université Lyon 1, ENS Lyon-5, Rue de La Doua, F-69100, Villeurbanne, France
[d] Barcelona Microelectronics Institute IMB-CNM (CSIC), Bellaterra, Spain

ARTICLE INFO

Keywords:
Electrochemical biosensor
Mott-Schottky
Silicon nitride transducer
Tumour Necrosis Factor
Human artificial saliva

ABSTRACT

In the present study, we have developed a capacitance electrochemical biosensor based on silicon nitride substrate (Si3N4/SiO2/Si[P]/Al) for Tumour Necrosis Factor Alpha (TNF-α) cytokines detection. Micro-contact printing, Fluorescence microscopy characterization and contact angle measurement (CAM) were carried out during the bio-functionalization of the biosensor surface. Mott-Schottky analyses were applied for TNF-α detection within the range of 1 pg/mL to 30 pg/mL in which the immunosensor has exhibited a good linearity, a sensitivity of 4 mV.pM^{-1} and 4.4 mV.pM^{-1} in PBS and artificial saliva (AS) respectively. While the LOD was found at 0.38 pg/mL and 1 pg/mL in PBS and AS respectively. The developed immunosensor has also demonstrated a high and good selectivity for TNF-α detection in human AS when compared to other interferences like Cortisol and Interleukin-10. The performances of the developed biosensor are very promising for biomedical application to predict the first sign of inflammation.

1. Introduction

Classical analyses for patients suffering from chronic disease were generally made by analysing blood or human plasma [1]. This was considered as very stressful and invasive analyses especially for elderly patients. During the last few decades, several challenges have aroused the interest of scientific researchers for chronic disease monitoring trough non-invasive approaches for patient's suffering from heart failure (HF). For this interest, critical biomarkers secreted during local and systemic inflammation were analysed in human saliva taking into account the advantages of painless, multiple sample collections by unskilled people, real-time monitoring, non-invasive, and especially stress-free collection for the patient, etc [2–6]. Human saliva contents reflect our body's health and about 20% of blood proteins are also present in saliva [7]. Besides, numerous studies had also proved that the concentration of TNF-α in saliva reflect those in blood [8,9]. Tumour necrosis factor-alpha (TNF-α), widely considered as one of the biomarkers detected during the acute stage of inflammation in both blood and saliva [10]. Nowadays, TNF-α is considered as an indicator biomarker for HF diagnosis [11]. HF is becoming a priority global health concern, affecting around 26 million people worldwide [12] and is estimated to possess about 26.819 $ as a lifetime cost for HF patients [13]. Although there is no cure for HF disease [14], however, early diagnosis can allow to take care of patients very quickly and to improve their health state.

Several techniques have been tested and used to quantify and detect TNF-α and other biomarkers to predict the first signs of inflammation [15,16]. Enzyme-linked immunosorbent assays (ELISA) [17,18], bioassays [19], radio-immunoassays (RIA) [20], surface plasmon resonance [21] and other methods [22–27] were widely used in this interest and are considered as standard methods. Although, most of these techniques are accurate and provide rapid screening and multiple analyses; they still limited by the high cost and the necessity of a qualified person to carry these analyses. To overcome the beyond limitations and satisfy the need of medical tools with high sensitivity, linear response, low cost and especially a low limit of detection, many scientific researchers have developed various strategies for biomarkers detection in human saliva. This latter contains a broad spectrum of biomarkers including TNF-α, cortisol, interleukin-10 [28] and N-terminal proB-type natriuretic peptide (NT-proBNP) [6], and their detection

* Corresponding author.
E-mail address: a.baraket@gmail.com (A. Baraket).

https://doi.org/10.1016/j.talanta.2019.120501
Received 24 July 2019; Received in revised form 19 October 2019; Accepted 23 October 2019
Available online 23 October 2019
0039-9140/

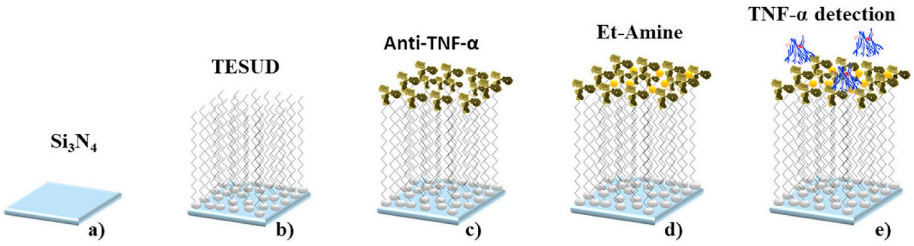

Fig. 1. Schematic illustrations of the chemical surface modification and bio-functionalization process of the immunosensor with antibodies *Anti*-TNF-α. a) Si_3N_4 surface cleaning and activation. b) Si_3N_4 surface functionalization with TESUD. c) *Anti*-TNF-α antibodies immobilization step d) Si_3N_4 surface blocking using 1% ethanolamine. e) Electrochemical TNF-α detection step.

may afford relevant information's for clinical diagnosis [2,29]. In addition, TNF-α concentrations in blood for healthy humans are generally below 40 pg/mL [38], while more than 80% of patients with severe autoimmune diseases may maintain between 10 and 300 pg/mL [39]. For patients suffering from chronic HF have an increased circulating level of TNF-α [40], tie with the severity of disease [41]. Recently TNF-α cytokine was detected by electrochemical biosensors which were widely used in the literature for biomarkers detections in saliva, urine and blood serum [30–32]. These electrochemical biosensors are considered as a promising tool since they can be easily miniaturized and require a small sample volume [33,34].

In the present study, we report the development of a capacitance electrochemical biosensors for TNF-α detection based on silicon nitride transducer (Si_3N_4). This material based micro-fabrication technology has been combined with biochemistry [35], allowing the fabrication of novel biosensing devices with great selectivity and good sensitivity [36]. Antibodies *Anti*-TNF-α were addressed onto the Si_3N_4 surface through covalent bonding of the aldehyde-silane (11-(triethoxysilyl) undecanal) TESUD. The fabricated biosensor has exhibited an enhanced response for TNF-α within a concentration range of 1–30 pg/mL, with a LOD of 1 pg/mL. Additional tests were carried out to investigate the immunosensor selectivity in both PBS and artificial saliva (AS) using IL-10 and cortisol as interferences [4], which might be both detected in saliva [37].

2. Material and methods

2.1. Reagents and chemicals

Antibodies *Anti*-TNF-α (Ab-TNF-α), TNF-α protein (TNF-α), Interleukin-10 (IL-10), and hydrocortisone (Cortisol) were purchased from Abcam (France). ((11-Triethoxysilyl)Undecanal TESUD), octadecyltrichlorosilane (OTS), ethanol (98%), potassium chloride (KCl), sodium phosphate dibasic (Na_2HPO_4), calcium chloride ($CaCl_2$), phosphate buffer solution (PBS) tablets, pure ethanol, urea and mucin were all purchased from Sigma-Aldrich. Acros Organics (France) supplied the sodium chloride. Ethanolamine (ETA), sulfuric acid (98%) (H_2SO_4) and hydrogen peroxide (30%) (H_2O_2) were purchased from Fluka (France). The polydimethylsiloxane (PDMS) was supplied from Dow Corning (France).

2.2. Silicon nitride transducer (fabrication process)

The (Al/Si-p/SiO_2/Si_3N_4) transducer was fabricated by using < 100 > silicon wafer orientation as substrate. The fabrication process was carried out in Centre National de MicroelectrÒnica (CNM-IMB, CSIC, Spain). The Si-p wafer was firstly doped with boron (1×10^{15}/cm^2) and afterwards was thermally oxidized at 850 °C to get 78 nm of SiO_2. Moreover, a thin layer of 100 nm thickness of Si_3N_4 was deposited onto SiO_2 by low-pressure chemical vapour deposition (CVD). Afterwards, 1 μm of aluminium was deposited on the backside of the wafer as an Ohmic contact [38]. Finally, the wafer was diced to individual squares of 1.2 cm^2 to be used as transducer of the biosensor.

2.3. Transducer bio-functionalization

Firstly, the silicon nitride substrates were cleaned by sonication in acetone for 15 min and then in ethanol for 15 min, then washed with distilled water and dried with nitrogen. This step was necessary to remove all organic contaminations provided from the remained protective resin layer. Then, the silicon nitride surface was activated with piranha solution ($1/3H_2O_2$; $2/3H_2SO_4$) for 30 min by keeping the electrode backside (Aluminum layer) outward from the piranha solution to protect it from wet etching [38]. The activation step was used to generate the silanol and silylamine groups [39], which are necessary to obtain a perfect adhesion of bio/chemical substances onto the silicon nitride surface (Fig. 1a). The obtained substrates were functionalized using 1% TESUD in ethanol solution overnight, rinsed gently with ethanol, dried with nitrogen and left in the oven at 100 °C for 1 h. Therefore, self-assembled monolayers (SAMs) of aldehyde-silane were formed onto the Si_3N_4 surface (Fig .1.b). The monoclonal *Anti*-TNF-α antibodies were covalently bonded to the surface through the acid amine linkage. So, after 3 h of incubation of antibodies TNF-α at room temperature (20 ± 2 °C) (Fig. 1c), the residual activated carboxylic acid groups of TESUD were blocked using 1% of ethanolamine diluted in PBS for an additional 30 min in order to reduce the nonspecific binding during the detection process [40] (Fig. 1d). Finally, the samples were neatly rinsed with PBS using micropipette and were ready for TNF-α detection step (Fig. 1e).

2.4. Micro-contact printing and fluorescent microscopy

Micro-contact printing (μCP) technique was used for checking the successfully bio-functionalization surface and to ensure that the TNF-α antibodies were perfectly bonded onto the TESUD modified silicon nitride surface. The detailed process of μCP technique was previously published in our group [41]. Briefly, a negative elastomeric stamp based on polydimethylsiloxane (PDMS) with patterns of squares 10 μm^2 was fabricated by replica moulding. Here, the pre-polymer PDMS and curing agent were mixed with a ratio of (10:1 w/w) respectively. Then the mixture was casted onto a positive silicon mould with micropillars on relief of its surface. The PDMS stamp was inked with OTS (5 μM) for 1 min and brought in conformal contact with the activated silicon surface. After peeling off the PDMS, a SAMs of OTS were formed on the silicon nitride surface as a blocking layer (Fig. 2A). The obtained substrate was then immersed in ethanol solution with 1% of TESUD for 30 min, rinsed gently with ethanol, dried with a slight stream of nitrogen and placed in the oven for 1 h at 100 °C for chemisorption of both silane OTS and TESUD.

Afterwards, *Anti*-TNF-α antibodies were immobilized onto TESUD, followed by Ethanol-Amine deactivation as previously described (Fig. 2B). The immunosensor was then incubated in PBS with 10 pg/mL of TNF-α cytokines for 30 min to allow the antibodies-antigens interaction. Then, the biosensor was rinsed with PBS to remove the unbounded TNF-α cytokines and incubated again with antibodies *Anti*-TNF-α labelled with Rhodamine (Rh) for 1 h to form a sandwich antibody-cytokine-antibody@Rh (Fig. 2B). Finally, the sample was rinsed with distilled water and dried with nitrogen for fluorescence microscopy characterization.

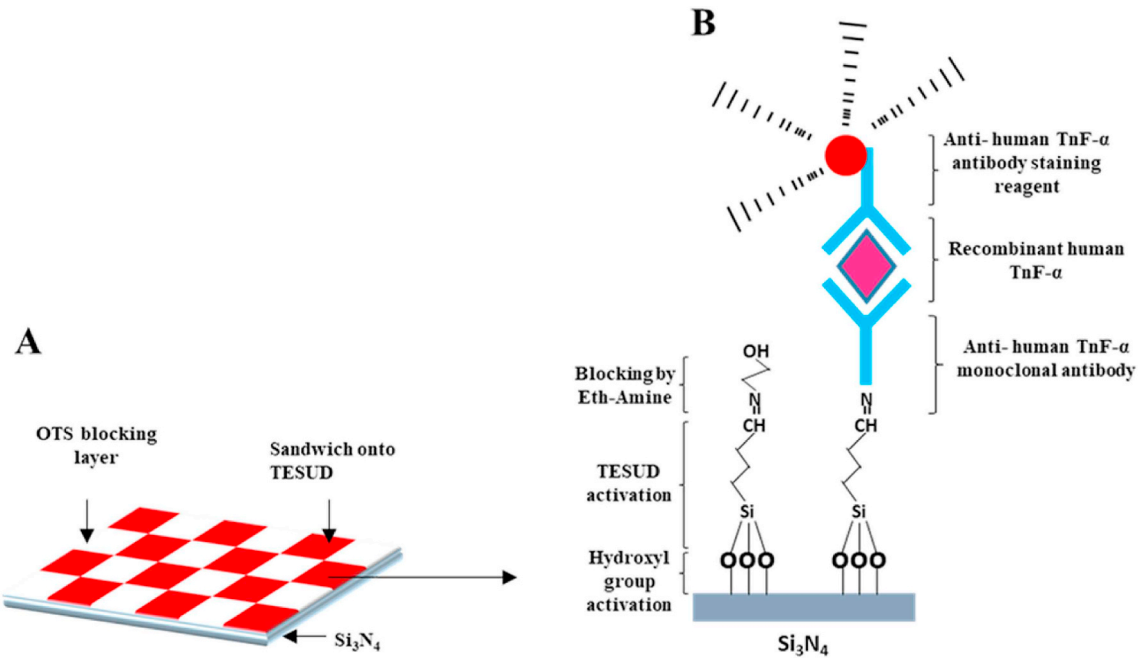

Fig. 2. A) Illustration of TESUD and OTS pattern after μCP B) illustration of sandwich formation antibody-cytokine-antibody@Rh

Fluorescence microscopy (Zeisaxioplan 2 imaging apparatus, equipped with a monochrome camera, 10x and 40x lenses) was used to take the fluorescence images. Samples (positive and negative tests) were observed by fluorescent light. Antibodies *Anti*-TNF-α labelled with Rhodamine (Rh) were excited with a 550 (± 25) nm band-pass filter and fluorescence from the sample was observed with a 605 (± 70) nm band-pass filter.

2.5. Contact angle measurements

Data Physics Instruments digidrop (Germany) has been used to measure the contact angle measurements (CAM). A droplet of 5 μL of deionized water was deposited on the silicon nitride surface, and the CAM was applied after each chemical surface modification. Five CAM were recorded for each chemical modification step.

2.6. Antigen dilution and artificial saliva preparation

The antibodies *Anti*-TNF-α, cytokines TNF-α, IL-10, and Cortisol have been reconstituted following the protocol of the supplier in PBS (10 mM, pH 7.4) and aliquoted at 20 μL to get a final stock with a concentration of 125 μg/mL, 33 μg/mL, 10 μg/mL and 50 μg/mL respectively. Our standard solutions of the TNF-α cytokines as well as the interferences IL-10 and Cortisol were prepared within the same range of concentration of 1 pg/mL to 30 pg/mL by dissolving the appropriate quantity of cytokines in PBS (10 mM, pH 7.4). The same procedure was used for the AS test by dissolving the appropriate amount of cytokines stock solution in AS. This latter was accurately prepared by dissolving in 200 mL 0.12 g of Na_2HPO_4, 0.12 g of $CaCl_2$, 0.08 g of KCL, 0.08 g NaCl, 0.8 g of mucin and 0.8 g of urea in deionized water [28]. The pH of the obtained solution was gradually adjusted to 7.4 by appending NaOH and finally aseptically stored at −4 °C until use.

2.7. Mott-Schottky analysis

A three-electrode system has been used for electrochemical detection by using; a platinum counter electrode (Pt), a silver/silver chloride (Ag/AgCl) reference electrode and the biosensor acted as a working electrode. This latter was sandwiched between two parts of a conventional 1 mL electrochemical Teflon cell. Electrical contact was taken from the backside of the biosensor [41,42]. The Mott Schottky experiments were associated with a VMP3 potentiostat monitored by EC-Lab software (Biologic Science Instruments, France). The Mott-Schottky analyses were performed by sweeping the potential from −0.5 V to +4 V at a constant frequency of 10 KHz and a step rate of 25 mV. All the measurements were carried out in PBS (10 mM, pH 7.4) and in AS with a constant pH = 7.4, at room temperature (20 ± 2 °C) inside a Faraday cage.

3. Results and discussion

3.1. Contact angle measurements

Contact angle measurements (CAM) were used after each chemical surface modification of the transducer in order to follow the hydrophilic property of the surface and thus check the successful chemical functionalization of the silicon nitride Si_3N_4 surface. The CAM results were summarized in Fig. 3, and illustrate the CAM evolution as a function of chemical surface modification. The CAM of bare Si_3N_4 surface was recorded at 60.7° (Fig. 3a), which is in a good agreement with the literature results [43]. The CAM has decreased to 33.7° (Fig. 3b) after piranha activation due to the hydroxyl groups formed onto the silicon nitride surface. Afterwards and after functionalization with TESUD, the CAM has increased again to 56.3° (Fig. 3c) highlighting thus the hydrophobic character of TESUD due to its hydrocarbon chain.

3.2. Fluorescence characterization

Fluorescence characterization has been used as a rapid tool to ensure the bio-recognition process between the antibodies *Anti*-TNF-α and its corresponding cytokines TNF-α. This latter has been sandwiched between the first antibody *Anti*-TNF-α previously immobilized onto Si_3N_4 and the second antibody labelled with Rhodamine *Anti*-TNF-α@Rh to form a sandwich Anti- TNF-α < TNF-α > *Anti*-TNF-α@Rh (Fig. 2B). The rhodamine outward from the surface indicates the well formation the sandwich and thus the successful biorecognition.

The μCP has been used to create the required pattern through the PDMS stamp as previously described. Here the sandwich Anti- TNF-

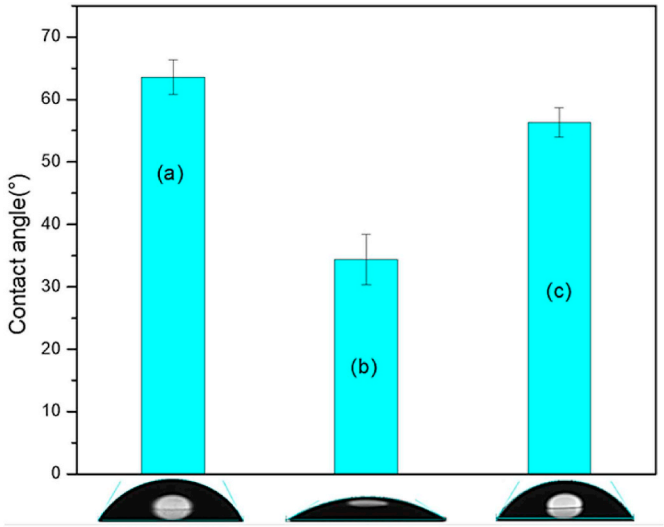

Fig. 3. CAM and images of water droplet evolution as a function of chemical surface modification of (a) bare Si_3N_4 surface after acetone and ethanol cleaning, (b) after piranha oxidation (c) and after TESUD formation.

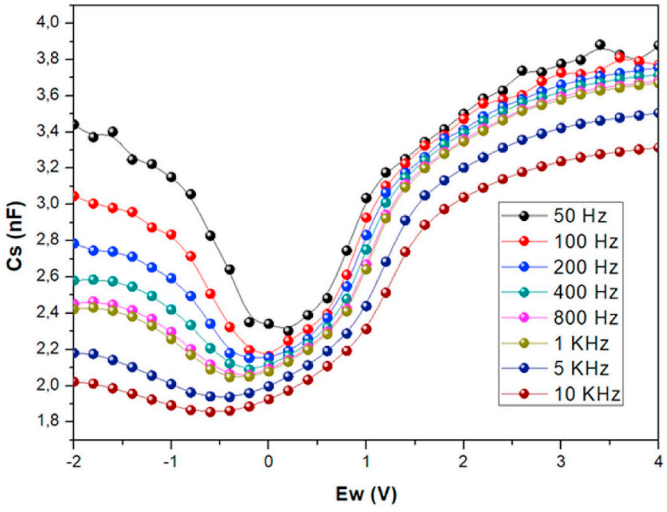

Fig. 5. Capacitive measurements as a function of the applied potential for different frequency ranges.

α < TNF-α > *Anti*-TNF-α@Rh (red squares Fig. 4A) will be formed only onto the patterns previously functionalized with TESUD. Fig. 4A shows a homogenous pattern of the fluorescent *Anti*-TNF-α@Rh and demonstrates the successful immobilization of *Anti*-TNF-α antibodies onto Si_3N_4 and also the successful detection of TNF-α. No fluorescence was observed onto the blocked area with OTS which indicate the absence of nonspecific adsorption. Negative tests were made to prove that what was observed in the first test was well the biorecognition and not the only adsorption. The same procedure of sandwich was repeated by using this time IL-10 cytokines instead of TNF-α. Here no fluorescent has been observed as there was no recognition process (Fig. 2B).

This fluorescence test was made before electrochemical detection to prove that what will be detected is well the biorecognition between *Anti*-TNF-α antibodies and their corresponding cytokines TNF-α and not the nonspecific adsorption.

3.3. Mott-Schottky results

3.3.1. Electrochemical parameters optimisation

Mott-Schottky analyses have been used to study the semiconducting behaviour of our biosensor based on silicon nitride substrate after TESUD functionalization and *Anti*-TNF-α immobilization. The capacitance measurements as a function of the applied potential with different frequencies ranging from 50 Hz to 10 KHz curves recorded in PBS buffer solution were presented in Fig. 5. The capacitance responses were typical with the appearance of the three known regions: the accumulation, the depletion and the inversion regions [41]. This test has been done to optimize the frequency and the potential, which were two specific and significant parameters for the Mott-Schottky analysis technique. The final potential range and frequency were chosen from −0.5 V to 2.5 V and at 10 KHz respectively as it gives a better capacitance behaviour.

3.3.2. Detection and interference study of TNF-α in PBS

The detection of TNF-α cytokines at various concentrations was presented in Fig. 6A. Here, the capacitance response was normalized by dividing the capacitance of the substrate value (Cs) by the minimum value (C_{min}) of each measurement curves of C (V). The Capacitance response was presented as C_s/C_{min} in function of the applied potential of the working electrode (Ew). The first curve from left to right (Fig. 6A), corresponds to the biosensor with *Anti*-TNF-α before any detection. The biosensor was then left within the cell and was incubated in 1 pg/mL of TNF-α cytokines in PBS at 4 °C for 30 min. Then, the biosensor was rinsed gently with PBS to remove the excess of the cytokine TNF-α adsorbed onto the surface. Finally, the Teflon cell with the biosensor was placed again inside the faraday box for Mott-Schottky analyses (Fig. 6A). Here the second curve corresponding to 1 pg/mL has shifted from the first showing thus a difference of potential equivalent to a flat band voltage variation. By increasing the TNF-α concentration, the flat band voltage increases, also showing the detection phenomenon. The biosensor sensitivity was then obtained by measuring the slope of the potential variation in function of TNF-α cytokines concentration.

Fig. 6.B illustrates the calibration curve of the biosensor within a

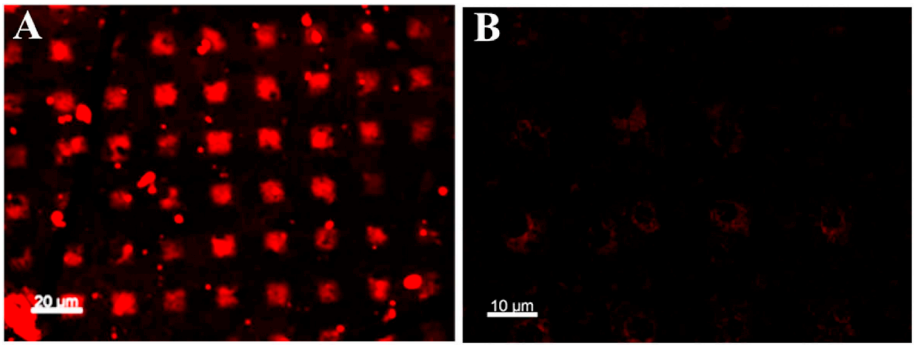

Fig. 4. Fluorescent images of A) the successful formation of the sandwich Anti- TNF-α < TNF-α > *Anti*-TNF-α@Rh and B) negative test by using IL-10 instead TNF-α cytokines.

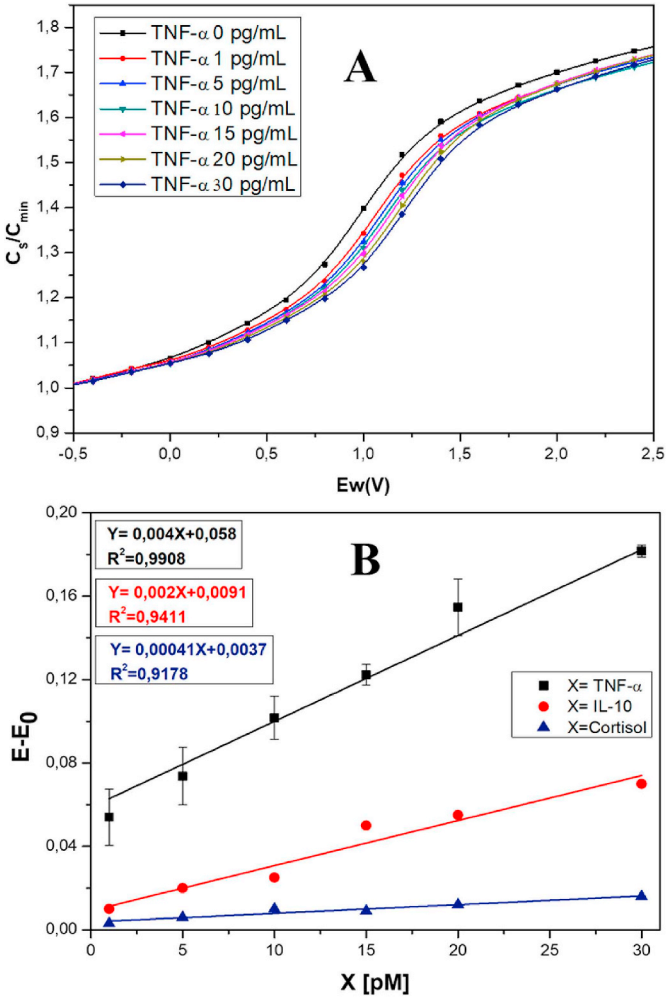

Fig. 6. (A) Mott-Schottky plots of TNF-α detection in PBS, **(B)** the detection sensitivity curves of TNF-α, IL-10 cytokines and cortisol in PBS.

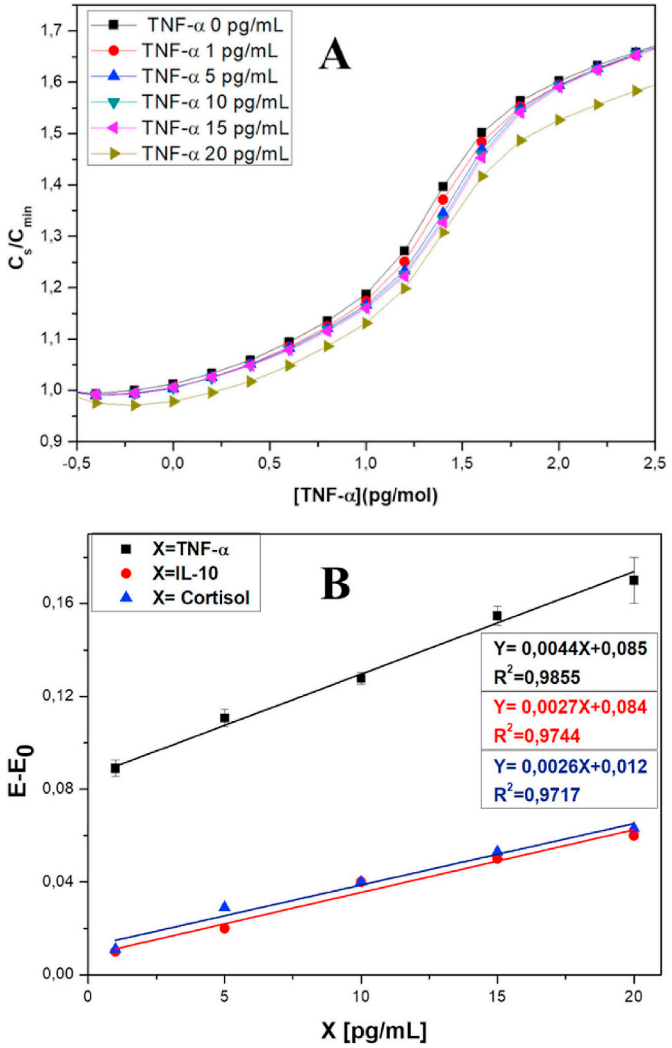

Fig. 7. (A) Mott-Schottky plots of Ag-TNF-α detection in AS, **(B)** detection sensitivity curves of Ag-TNF-α, IL-10 cytokine and cortisol in AS.

linear range of 1–30 pg/mL of TNF-α. E_0 is the potential of *Anti*-TNF-α without any cytokine concentration, and E is the extracted potential of different TNF-α concentration utilizing the tangential method. The fabricated biosensor provides a good sensitivity of 4 mV/pM and a correlation coefficient of 0.99. The LOD was calculated as 3.3xSD/slope and was found at 0.38 pg/mL. The specificity of the developed biosensor was also studied by using IL-10 and Cortisol instead TNF- α through the same structure and the same experimental process based on TESUD/*Anti*-TNF-α antibodies immobilization. The detection of the two interferences was made within the same linear range of TNF-α cytokines. The potential variation of IL-10 and Cortisol shows the specificity and sensitivity of the biosensor for TNF-α when compared to the interference.

Until this stage, the interactivity of the developed biosensor and cytokines detection was achieved in PBS. In order to explore more the performances of the immunosensor, Mott-Schottky analysis was carried out in AS.

3.3.3. Detection and interference study of TNF-α in artificial saliva

Different concentrations of TNF-α (1, 5, 10, 15 and 20 pg/mL) were prepared directly in AS instead PBS. The biosensor was then incubated for each concentration and followed by Mott-Schottky analysis for each concentration as previously described. Here, the working electrode was again sandwiched within the same Teflon cell and filled with 1 mL of PBS as electrolyte solution for electrochemical analyses. The normalized capacitance response (Cs/Cmin) as a function of the applied potential for different TNF-α concentrations was presented in Fig. 7A. The evolution of the difference of flat band voltage variation as a function of cytokines concentration highlights the detection phenomenon in AS.

The calibration curve of TNF-α detection shows a linear regression equation $(E\text{-}E_0) = 0.0044[\text{TNF-}\alpha] + 0.085$ and an $R^2 = 0.985$ (Fig. 7B). The same study was also repeated with both interferences IL-10 and Cortisol in AS. Here the biosensor was slightly more sensitivity toward TNF-α cytokines with a LOD of 1 pg/mL (with a sensitivity of 4.4 $mV.pM^{-1}$ and an $R^2 = 0.985$) when compared to IL-10 (with a sensitivity of 2.7 $mV.pM^{-1}$ and an $R^2 = 0.974$) and Cortisol (with a sensitivity of 2.6 $mV.pM^{-1}$ and an $R^2 = 0.971$).

Table 1 lists a comparative study of different LOD reached, linear range and the technique used reported in the literature to measure TNF in both artificial and human saliva samples.

Although the developed biosensor did not exhibit the best limit of detection as presented in Table 1, however, it is still, an active competitor to the gold transducer in term of protocol complication and stability material.

4. Conclusion

The present study aimed to explore the development of a novel capacitance electrochemical biosensor based on $Si_3N_4/SiO_2/Si/Al$

Table 1
Comparison of different electrochemical immunosensors for TNF- α detection.

Technique used	Analyte	Linear range	LOD	Reference
Impedance spectroscopy	Artificial saliva	1–100 pg/mL	1 pg/mL	[28]
Amperometry	Artificial saliva	1–30 pg/mL	1 pg/mL	[4]
Amperometry	Artificial saliva	1–15 pg/mL	0.3 pg/mL	[44]
Impedance spectroscopy	PBS	0.01–2 pg/mL	3.7 fg/mL	[45]
Differential pulse voltammetry	Serum	0–1000 ng/mL	37 ng/mL	[46]
potentiometric	Serum	0.1–1 mg/L	0.015 mg/L	[47]
Amperometry	Saliva	1–200 pg/mL	0.85 pg/mL	[48]
Impedimetric	Artificial saliva	1–15 pg/mL	1 pg/mL	[5]
Mott Schottky	Artificial saliva	1–30 pg/mL	1 pg/mL	This work

structure utilizing Mott-Schottky analysis for the specific detection of TNF-α. Silicon nitride was used in this study to its known high stability in the literature, and it starts to become a good competitor to the gold transducer. Here, and under optimized conditions, the developed electrochemical capacitance biosensor provides a high sensitivity of 4 $mV.pM^{-1}$ and 4.4 $mV.pM^{-1}$ in PBS and in AS respectively and LOD of 0.38 pg/mL and 1 pg/mL in PBS and AS respectively. The immunosensor was highly selective in PBS when compared to AS. The selectivity degradation in AS compared might be explained by the matrix effect of saliva composition, which prevents the specific detection of TNF-α. Therefore, magnetic nanoparticles could be integrated in the future onto silicon nitride transducer [44,49,50] to enhance the sensitivity of this immunosensor within complex physiological mediums such as human saliva or blood samples.

Acknowledgements

The authors acknowledge the financial support from the European project KardiaTool [Grant No. 768686].

References

[1] L.L. Patton, J.B. Epstein, A.R. Kerr, Adjunctive techniques for oral cancer examination and lesion diagnosis: a systematic review of the literature, J. Am. Dent. Assoc. 139 (2008) 896–905 quiz 993–4 http://www.ncbi.nlm.nih.gov/pubmed/18594075 , Accessed date: 16 July 2018.
[2] L.F. Hofman, Human saliva as a diagnostic specimen, J. Nutr. 131 (2001) 1621S–1625S, https://doi.org/10.1093/jn/131.5.1621S.
[3] F.G. Bellagambi, I. Degano, S. Ghimenti, T. Lomonaco, V. Dini, M. Romanelli, F. Mastorci, A. Gemignani, P. Salvo, R. Fuoco, F. Di Francesco, Determination of salivary α-amylase and cortisol in psoriatic subjects undergoing the Trier Social Stress Test, Microchem. J. 136 (2018) 177–184, https://doi.org/10.1016/j.microc.2017.04.033.
[4] L. Barhoumi, A. Baraket, F.G. Bellagambi, G.S. Karanasiou, M. Ben Ali, D.I. Fotiadis, J. Bausells, N. Zine, M. Sigaud, A. Errachid, A novel chronoamperometric immunosensor for rapid detection of TNF-α in human saliva, Sens. Actuators B Chem. 266 (2018) 477–484, https://doi.org/10.1016/j.snb.2018.03.135.
[5] A. Longo, A. Baraket, M. Vatteroni, N. Zine, J. Baussells, RogerFuoco, F. Di Francesco, G.S. Karanasiou, D.I. Fotiadis, A. Menciassi, A. Errachid, Highly sensitive electrochemical BioMEMS for TNF-α detection in humansaliva: heart failure, Procedia Eng 168 (2016) 97–100, https://doi.org/10.1016/J.PROENG.2016.11.156.
[6] J. Yong, Y. Foo, Y. Wan, K. Kostner, A. Arivalagan, J. Atherton, J. Cooper-white, G. Dimeski, C. Punyadeera, NT-ProBNP levels in saliva and its clinical relevance to heart failure, 7 (2012) 1–6, https://doi.org/10.1371/journal.pone.0048452.
[7] S. Hu, Y. Li, J. Wang, Y. Xie, K. Tjon, L. Wolinsky, R.R.O. Loo, J.A. Loo, D.T. Wong, Human saliva proteome and transcriptome, J. Dent. Res. 85 (2006) 1129–1133, https://doi.org/10.1177/154405910608501212.
[8] P. Gümüş, N. Nizam, D.F. Lappin, N. Buduneli, Saliva and serum levels of B-cell activating factors and tumor necrosis factor-α in patients with periodontitis, J. Periodontol. 85 (2014) 270–280, https://doi.org/10.1902/jop.2013.130117.
[9] G.A.S. Amer, A.M. El Refaei, A. El-latif, M. El-Balshy, D. Andrology, A Comparison between Serum and Salivary Tumor Necrosis Factor- Alpha in Oral Lichen Planus, (2009) https://www.semanticscholar.org/paper/A-Comparison-between-Serum-and-Salivary-Tumor-Alpha-Amer-Refaei/5286168dabd51c469e52f537beeb069e39da406b , Accessed date: 14 September 2019.
[10] B. Levine, J. Kalman, L. Mayer, H.M. Fillit, M. Packer, Elevated circulating levels of tumor necrosis factor in severe chronic heart failure, N. Engl. J. Med. 323 (1990) 236–241, https://doi.org/10.1056/NEJM199007263230405.
[11] Q. Javed, I. Murtaza, Therapeutic potential of tumour necrosis factor-alpha antagonists in patients with chronic heart failure, Heart Lung Circ. 22 (2013) 323–327, https://doi.org/10.1016/j.hlc.2012.12.002.
[12] O. Chioncel, S.J. Greene, M. Vaduganathan, The global health and economic burden of hospitalizations for heart failure lessons learned from hospitalized heart failure registries, J. Am. Coll. Cardiol. 63 (2014) 1123–1133, https://doi.org/10.1016/j.jacc.2013.11.053.
[13] W. Lesyuk, C. Kriza, P. Kolominsky-rabas, Cost-of-illness Studies in Heart Failure: a Systematic Review 2004 – 2016, (2018), pp. 1–11.
[14] P. Ponikowski, S.D. Anker, M.R. Cowie, T.L. Force, Heart Failure: Preventing Disease and Death Worldwide, (2014), https://doi.org/10.1002/2055-5822.12005.
[15] I. Subirana, O. Diaz, J. Vila, A. Francés, E. Delpon, Prediction of Coronary Disease Incidence by Biomarkers of Inflammation , Oxidation , and Metabolism, (2018), pp. 1–7, https://doi.org/10.1038/s41598-018-21482-y.
[16] J. Gassen, M.L. Prokosch, M.J. Eimerbrink, R.P.P. Leyva, J.D. White, J.L. Peterman, A. Burgess, D.J. Cheek, A. Kreutzer, S.C. Nicolas, G.W. Boehm, S.E. Hill, Inflammation predicts decision- making characterized by impulsivity , present focus , and an inability to delay gratification, Sci. Rep. (2019) 1, https://doi.org/10.1038/s41598-019-41437-1.
[17] J. Wang, G. Liu, M.H. Engelhard, Y. Lin, Sensitive immunoassay of a biomarker tumor necrosis factor-α based on poly(guanine)-functionalized silica nanoparticle label, Anal. Chem. 78 (2006) 6974–6979, https://doi.org/10.1021/ac060809f.
[18] M.W. van der Linden, T.W. Huizinga, D.J. Stoeken, A. Sturk, R.G. Westendorp, Determination of tumour necrosis factor-alpha and interleukin-10 production in a whole blood stimulation system: assessment of laboratory error and individual variation, J. Immunol. Methods 218 (1998) 63–71 http://www.ncbi.nlm.nih.gov/pubmed/9819123 , Accessed date: 6 July 2018.
[19] L.J. Jones, V.L. Singer, Fluorescence microplate-based assay for tumor necrosis factor Activity using SYTOX green stain, Anal. Biochem. 293 (2001) 8–15, https://doi.org/10.1006/abio.2001.5116.
[20] A.M. Teppo, C.P. Maury, Radioimmunoassay of tumor necrosis factor in serum, Clin. Chem. 33 (1987) 2024–2027 http://www.ncbi.nlm.nih.gov/pubmed/3677374 , Accessed date: 6 July 2018.
[21] J. Wang, A. Munir, H.S. Zhou, Au NPs-aptamer conjugates as a powerful competitive reagent for ultrasensitive detection of small molecules by surface plasmon resonance spectroscopy, Talanta 79 (2009) 72–76, https://doi.org/10.1016/j.talanta.2009.03.003.
[22] L. Luo, Z. Zhang, L. Ma, Determination of recombinant human tumor necrosis factor-α in serum by chemiluminescence imaging, Anal. Chim. Acta 539 (2005) 277–282, https://doi.org/10.1016/j.aca.2005.02.046.
[23] F. Berthier, C. Lambert, C. Genin, J. Bienvenu, Evaluation of an automated immunoassay method for cytokine measurement using the Immulite Immunoassay system, Clin. Chem. Lab. Med. 37 (1999) 593–599, https://doi.org/10.1515/CCLM.1999.092.
[24] A. Ogata, H. Tagoh, T. Lee, T. Kuritani, Y. Takahara, T. Shimamura, H. Ikegami, M. Kurimoto, K. Yoshizaki, T. Kishimoto, A new highly sensitive immunoassay for cytokines by dissociation-enhanced lanthanide fluoroimmunoassay (DELFIA), J. Immunol. Methods 148 (1992) 15–22, https://doi.org/10.1016/0022-1759(92)90153-K.
[25] U. Turpeinen, U.-H. Stenman, Determination of human tumour necrosis factor-α (TNF-α) by time-resolved immunofluorometric assay, Scand. J. Clin. Lab. Investig. 54 (1994) 475–483, https://doi.org/10.3109/00365519409085472.
[26] R.A. Evangelista, A. Pollak, E.F. Gudgin Templeton, Enzyme-amplified lanthanide luminescence for enzyme detection in bioanalytical assays, Anal. Biochem. 197 (1991) 213–224, https://doi.org/10.1016/0003-2697(91)90381-3.
[27] G.B. Hurst, M.V. Buchanan, L.J. Foote, S.J. Kennel, Analysis for TNF-α using solid-phase Affinity capture with radiolabel and MALDI-MS detection, Anal. Chem. 71 (1999) 4727–4733, https://doi.org/10.1021/ac9905423.
[28] F.G. Bellagambi, A. Baraket, A. Longo, M. Vatteroni, N. Zine, J. Bausells, R. Fuoco, F. Di Francesco, P. Salvo, G.S. Karanasiou, D.I. Fotiadis, A. Menciassi, A. Errachid, Electrochemical biosensor platform for TNF-α cytokines detection in both artificial and human saliva: heart failure, Sens. Actuators B Chem. 251 (2017) 1026–1033, https://doi.org/10.1016/j.snb.2017.05.169.
[29] Y.-H. Lee, D.T. Wong, Saliva: an emerging biofluid for early detection of diseases, Am. J. Dent. 22 (2009) 241–248 http://www.ncbi.nlm.nih.gov/pubmed/19824562 , Accessed date: 13 September 2019.
[30] P. Yáñez-Sedeño, S. Campuzano, J.M. Pingarrón, Pushing the limits of electrochemistry toward challenging applications in clinical diagnosis, prognosis, and therapeutic action, Chem. Commun. 55 (2019) 2563–2592, https://doi.org/10.1039/c8cc08815b.
[31] D. Brennan, P. Galvin, Flexible substrate sensors for multiplex biomarker

monitoring, MRS Commun. 8 (2018) 627–641, https://doi.org/10.1557/mrc.2018.134.
[32] E. Povedano, E. Vargas, V.R.V. Montiel, R.M. Torrente-Rodríguez, M. Pedrero, R. Barderas, P.S. Segundo-Acosta, A. Peláez-García, M. Mendiola, D. Hardisson, S. Campuzano, J.M. Pingarrón, Electrochemical affinity biosensors for fast detection of gene-specific methylations with no need for bisulfite and amplification treatments, Sci. Rep. 8 (2018) 1–11, https://doi.org/10.1038/s41598-018-24902-1.
[33] S.K. Arya, S. Bhansali, Lung cancer and its early detection using biomarker-based biosensors, Chem. Rev. 111 (2011) 6783–6809, https://doi.org/10.1021/cr100420s.
[34] A. Baraket, M. Lee, N. Zine, N. Yaakoubi, J. Bausells, A. Errachid, A flexible electrochemical micro lab-on-chip: application to the detection of interleukin-10, Microchim. Acta 183 (2016) 2155–2162, https://doi.org/10.1007/s00604-016-1847-y.
[35] K. Awsiuk, A. Bernasik, M. Kitsara, A. Budkowski, P. Petrou, S. Kakabakos, S. Prauzner-Bechcicki, J. Rysz, I. Raptis, Spectroscopic and microscopic characterization of biosensor surfaces with protein/amino-organosilane/silicon structure, Colloids Surfaces B Biointerfaces 90 (2012) 159–168, https://doi.org/10.1016/j.colsurfb.2011.10.017.
[36] Q. Liu, X. Tu, K.W. Kim, J.S. Kee, Y. Shin, K. Han, Y.-J. Yoon, G.-Q. Lo, M.K. Park, Highly sensitive Mach–Zehnder interferometer biosensor based on silicon nitride slot waveguide, Sens. Actuators B Chem. 188 (2013) 681–688, https://doi.org/10.1016/J.SNB.2013.07.053.
[37] J. Silva, M. Humberto, Cytokines , Cortisol , and Nitric Oxide as Salivary Biomarkers in Oral Lichen Planus: a Systematic Review, (2018), pp. 1–11.
[38] L. Barhoumi, A. Baraket, N.M. Nooredeen, M.B. Ali, M.N. Abbas, J. Bausells, A. Errachid, Silicon nitride capacitive chemical sensor for phosphate ion detection based on copper phthalocyanine – acrylate-polymer, Electroanalysis 29 (2017) 1–11, https://doi.org/10.1002/elan.201700005.
[39] B. Hajji, P. Temple-Boyer, J. Launay, T. do Conto, A. Martinez, pH, pK and pNa detection properties of SiO2/Si3N4 ISFET chemical sensors, Microelectron. Reliab. 40 (2000) 783–786, https://doi.org/10.1016/S0026-2714(99)00285-1.
[40] M. Lee, N. Zine, A. Baraket, M. Zabala, F. Campabadal, R. Caruso, M.G. Trivella, N. Jaffrezic-Renault, A. Errachid, A novel biosensor based on hafnium oxide: application for early stage detection of human interleukin-10, Sens. Actuators B Chem. 175 (2012) 201–207, https://doi.org/10.1016/j.snb.2012.04.090.
[41] M. Bougrini, A. Baraket, T. Jamshaid, A. El Aissari, J. Bausells, M. Zabala, N. El Bari, B. Bouchikhi, N. Jaffrezic-Renault, E. Abdelhamid, N. Zine, Development of a novel capacitance electrochemical biosensor based on silicon nitride for ochratoxin A detection, Sens. Actuators B Chem. 234 (2016) 446–452, https://doi.org/10.1016/j.snb.2016.03.166.
[42] F. Nessark, A. Zouaoui, A. Garcia-Cruz, A. Bonhomme, M. Lee, B. Nessark, N. Zine, P. Marote, J. Bausells, A. Baraket, A. Errachid, Fabrication of new polypyrrole/silicon nitride hybrid materials for potential applications in electrochemical sensors: synthesis and characterization, J. Macromol. Sci. Part A Pure Appl. Chem. 54 (2017) 827–834, https://doi.org/10.1080/10601325.2017.1336728.
[43] R. Rawal, S. Chawla, C.S. Pundir, An electrochemical sulfite biosensor based on gold coated magnetic nanoparticles modified gold electrode, Biosens. Bioelectron. 31 (2012) 144–150, https://doi.org/10.1016/j.bios.2011.10.007.
[44] L. Barhoumi, F.G. Bellagambi, F.M. Vivaldi, A. Baraket, Y. Clément, N. Zine, M. Ben Ali, A. Elaissari, A. Errachid, Ultrasensitive immunosensor array for TNF-α detection in artificial saliva using polymer-coated magnetic microparticles onto screen-printed gold electrode, Sensors (2019) 19, https://doi.org/10.3390/s19030692.
[45] E.B. Aydın, M. Aydın, M.K. Sezgintürk, A highly sensitive immunosensor based on ITO thin films covered by a new semi-conductive conjugated polymer for the determination of TNFα in human saliva and serum samples, Biosens. Bioelectron. 97 (2017) 169–176, https://doi.org/10.1016/j.bios.2017.05.056.
[46] G. Baydemir, F. Bettazzi, I. Palchetti, D. Voccia, Strategies for the development of an electrochemical bioassay for TNF-alpha detection by using a non-immunoglobulin bioreceptor, Talanta 151 (2016) 141–147, https://doi.org/10.1016/j.talanta.2016.01.021.
[47] R. Say, E. Birlik, Ö. Bic, U. Deniz, Nano anti-tumor necrosis factor-alpha based potentiometric sensor for tumor necrosis factor-alpha detection, Sens. Actuators B Chem. 209 (2015) 864–869.
[48] C. Salvo, A. Gonz, Analytica Chimica Acta Electrochemical immunosensor for simultaneous determination of interleukin-1 beta and tumor necrosis factor alpha in serum and saliva using dual screen printed electrodes modi fi ed with functionalized double e walled carbon nanotube, (2017), pp. 1–8, https://doi.org/10.1016/j.aca.2016.12.034.
[49] T. Jamshaid, E.T.T. Neto, M.M. Eissa, N. Zine, M.H. Kunita, A.E. El-Salhi, A. Elaissari, Magnetic particles: from preparation to lab-on-a-chip, biosensors, microsystems and microfluidics applications, TrAC Trends Anal. Chem. (Reference Ed.) 79 (2016) 344–362, https://doi.org/10.1016/j.trac.2015.10.022.
[50] N. Ben Messaoud, A. Ait Lahcen, C. Dridi, A. Amine, Ultrasound assisted magnetic imprinted polymer combined sensor based on carbon black and gold nanoparticles for selective and sensitive electrochemical detection of Bisphenol A, Sens. Actuators B Chem. 276 (2018) 304–312, https://doi.org/10.1016/j.snb.2018.08.092.